ASSESSMENT OF CORROSION BEHAVIOUR OF SOME ALUMINIUM ALLOYS VIA ELECTROCHEMICAL AND FREE CORROSION TESTS IN ACIDIC AND NEUTRAL ENVIRONMENTS

By **Lapo Gabellini,** Department of Chemistry, DCUS, University of Florence and Consorzio INSTM, Florence, Italy
Nicola Calisi, Stefano M. Martinuzzi, Rosa Taurino and **Stefano Caporali*,** Department of Industrial Engineering, DIEF, University of Florence and Consorzio INSTM, Florence, Italy

*Corresponding author. E-mail: stefano.caporali@unifi.it

The corrosion behaviour of four commercial aluminium alloys, extensively employed in engineering applications, was evaluated by means of electrochemical and free corrosion tests in order to compare their performances in both acidic and neutral environments. The electrochemical parameters obtained via cyclic potentiodynamic polarisation were compared with the corrosion features observed on these alloys after free corrosion tests. Different morphologies and damage extents were identified on these samples and upon the aggressive environment and the results were related to the chemical composition of the alloy and the corrosion and passivation mechanisms.

The reduced availability of primary mineral resources as well as the growing environmental concerns about mining and disposal of metal commodities make unavoidable the embracement of more sustainable consumption practices. In this optic the use of non-scarce mineral resources and the prevention of corrosion effects which extend the working life, is highly desired. For such reason, the use of aluminium alloys is currently experiencing a continuous increase for widespread applications. In some of them aluminium made items could be in contact with human skin such as robotic surgery, rehabilitation equipment, watchmaking etc. Therefore, for these applications, the corrosion behaviour in acidic complex environments such as human sweat is of paramount importance. Corrosion behaviour is currently assessed by means of accelerated and/or electrochemical-based tests [1-4] which can provide, in a very short time, evidence about the corrosion tendencies [4-11].

Cyclic potentiodynamic polarisation (CPP) technique, is one of these techniques and probably the most suitable to investigate materials with active/passive behaviour and, more in general, localised corrosion phenomena [12,13]. Despite the high versatility, results of CPP are affected by several experimental parameters [14-17] needing an appropriate experimental set-up, as described in the ASTM G61 test [5].

In principle, by means of CPP, it is possible to detect the potential value at which the passive layer become unstable and undergoes severe damage [18], but it also can give mechanistic information about the corrosion phenomena [19]. That may be used to rank the corrosion tendency of metallic materials [4,19-22]. In CPP the potential scan usually starts near the open circuit potential (OCP) value and reaches an anodic potential than, the scan is reversed and stopped close to the cathodic potential at which the current changes sign from anodic to cathodic [19]. The current values at which the scan is reversed (i_{rev}) may be dependent on the nature of the analysed material and generally, 5mAcm^{-1} is considered a suitable value [21]. It is well known that discrepancies between free corrosion and electrochemical tests can be present in case of passive materials. That is related to the stability and recovery capability of the passive layer. Indeed, the backward or reverse scan, may present some peculiar features that are directly connected to the tendency of a material to undergo pitting or SCC corrosion [14,24,25]. Previous studies have investigated the processes taking place during the reverse scan aiming to rationalise the experimental data [14,21-26]. However, even if many electrochemical parameters are easily achievable, their physical meaning is not always straightforward. Just to say one, the sign of the hysteresis loop was proposed as related to surface acidification [16] or to the incipit of localised corrosion [27]. Regarding the pit transition potential (E_{ptp}) it was found to be practically unaffected by environment conditions [15] while, the difference between pitting potential (E_{pit}) and E_{ptp} is dependent to the pit micro chemical environment, and it could be used as an indicator of pitting susceptibility [21]. Some studies have compared the data obtained from CPP with the data from free corrosion tests [22] but, to the best of our experience, these are limited to neutral saline environments and no data are available for artificial sweat. In this work we compare corrosion behaviour of aluminium alloys in neutral and artificial sweat environments using both electrochemical and free corrosion approaches.

Experimental procedures

Samples preparation and inspection

Samples consisting of 1 mm thick 25x25 mm tokens of commercially available aluminium alloys (chemical composition as determined by XRF-WDS (Rigaku ZSX Primus II) is depicted in **Table 1**) were polished with emery paper down to 1200 grit, rinsed in distilled water, acetone and then air dried.

Alloy designation	Composition (w%)									
	Si	Fe	Mn	Mg	Cu	Zn	Cr	Ti	V	Al
AA1200A	0.46	0.29	n.d.	0.25	n.d.	n.d.	n.d.	n.d.	n.d.	99%
AA5182-O	0.13	0.26	0.39	4.4	0.06	0.01	0.01	0.02	0.01	balance
AA6008	0.64	0.2	0.12	0.47	0.18	n.d.	n.d.	n.d.	0.07	balance
AA6351 - T6	0.85	0.27	0.71	0.45	0.04	0.07	n.d.	n.d.	n.d.	balance

Table 1. Designation, chemical composition (Wt%) and hardness of the 4 commercial alloys tested.

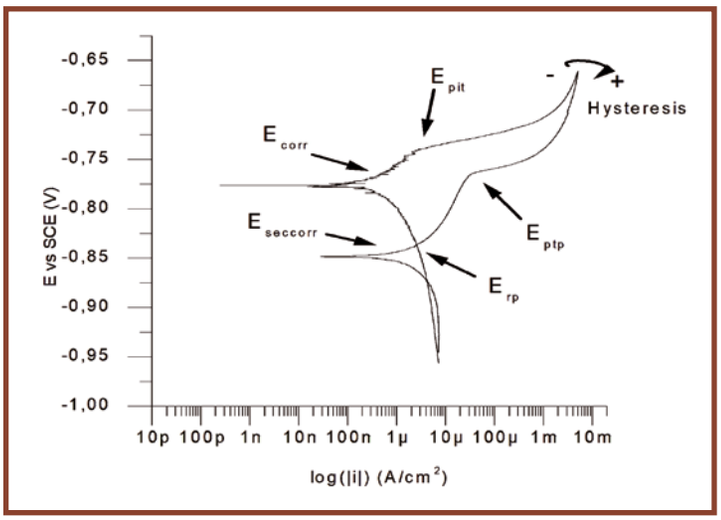

Figure 1 - Typical CPP curve with indication of the parameters taken into consideration in this work. E_{corr} is corrosion potential, E_{pit} is pitting potential, E_{ptp} is pit transition potential or the change in slope during the backward scan, E_{rp} is the repassivation potential or the potential at which inward and backward scan crosses, $E_{seccorr}$ identified at the current's change in sign during the backward scan.

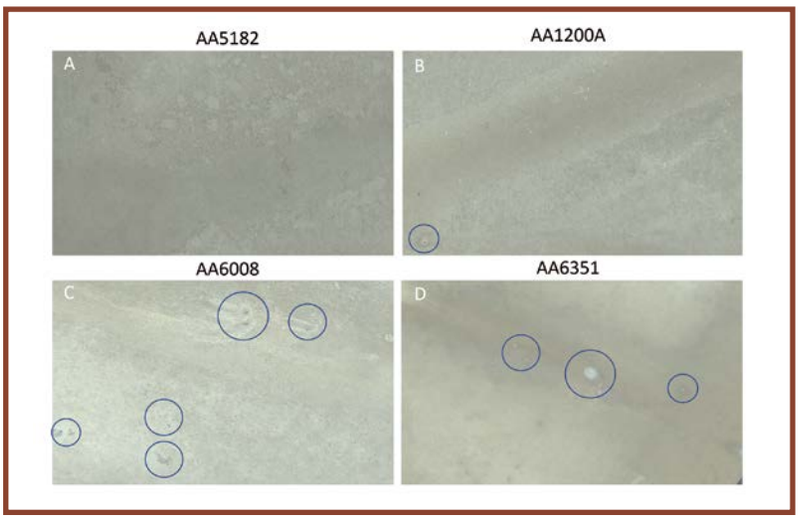

Figure 2 - Digital macro images of sample surface after salt spray test for 28 days. Blue circles identify the main corrosion features detectable.

After exposure to aggressive environments, the samples were washed with demineralized water, air dried and investigated by means of digital magnifier (OCULUX Macro Zoom, Microconsult), optical microscope (Nikon eclipse LV 150 NL) and scanning electron microscope (SEM, HITACHI 2300).

Free corrosion tests

Free corrosion tests were carried out in triplicate (three samples for each alloy) via both salt spray and contact modes. Salt spray test was achieved using a spray cabinet (Angelantoni model DCTC600) employing a 1L/h flux of nearly neutral saline solution containing 5% w/w NaCl at 35 °C. The control was performed at 24h, 48h, 96h and 7, 14, 21, 28 days (end of the test). Contact tests were performed in artificial sweat obtained by dissolving 5g/L of Urea, 20g/NaCl, 17.5g/L NH_4Cl, 2.5mL/L acetic acid, 15mL/L (S)-lactic acid in deionized water and the pH is adjusted to the value of 4.7 with a solution of 80 g/L of NaOH (analaR Normapur). The tests were realised in a home-built climatic chamber capable of maintaining 50 °C (±2 °C) and 100% relative humidity, by placing the samples on a cotton swab soaked with artificial sweat and located in a Petri dish. One of the two surfaces was exposed to the condensing vapours while the other was in contact with the cotton swab. The corrosion features check was done at 24 and 48 hours (end of the test).

Electrochemical tests

A computer controlled potentiostat (Autolab, Metrohm) controlled via Nova electrochemical software (2.1) and a three-electrode corrosion cell (EG&G Parr Flat cell) constituted the electrochemical set-up. Samples alloy constitute the working electrode, 1 cm^2 exposed area, while a platinum grid and a saturated calomel electrode (SCE) constituted counter and reference electrodes, respectively. All the tested samples reached stable potential with a variation smaller than 5mV/min within 600 seconds and cyclic polarisation curves (CPPs) were recorded at a scan rate of 0.1667mV/s from -0.2V vs OCP up to the potential's value corresponding to a current of 5 mA/cm^2 were the scan was reversed. In artificial sweat solution, the CPP curves were performed from -0.2V vs OCP toward an anodic direction until 15 mA current is reached, then the scan is reversed. The experimental parameters obtained from such experiments are schematized in **Figure 1**.

Results

Salt spray free corrosion tests

Representative images of the sample surface after 28 days of exposure are depicted in **Figure 2**. All the samples but AA5182 showed a rapid onset of corrosion pits whose number increases as a function of the exposure time, leading to a marked change in surface's appearance. There are significant differences among the tested alloys, from which the following rank AA6008 > AA6351 > AA1200A > AA5182 can be defined. The most performing alloy (AA5182) displays only few small pits compared to the other alloys, as evidenced in Figure 2 and **Figure 3**.

Artificial sweat solution

As expected, in artificial sweat, the corrosion features become more evident than in the neutral environment. Just after 48 hours the samples present large areas macroscopically stained and visibly damaged (**Figure 4**).

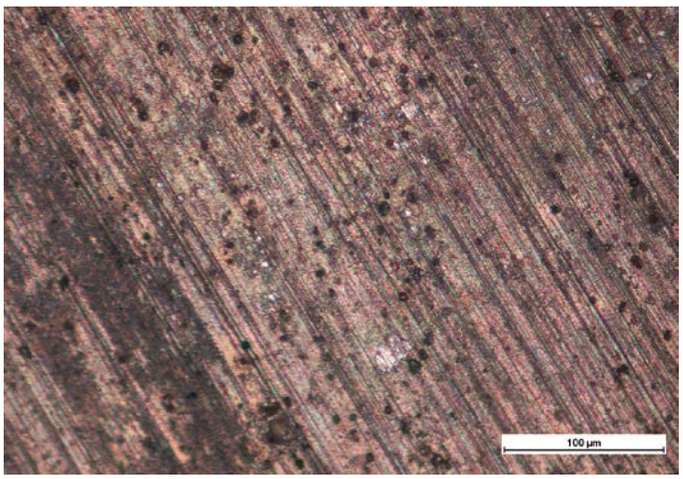

3 - Optical microscope images comparing the surfaces of AA5182 (left) and AA6008 (right) samples after 4 weeks of NSS. Ruler size, 200 µm.

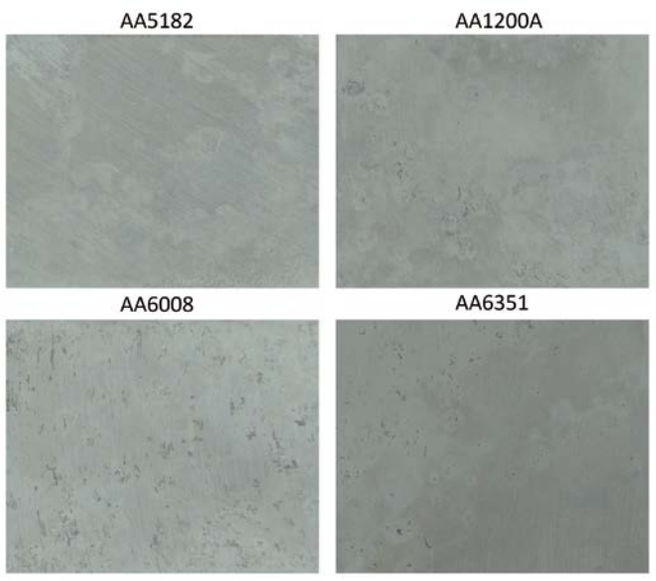

4 - Optical examination of samples surface after 48h exposure to artificial sweat. AA5182 alloy resulted the less affected by corrosion phenomena.

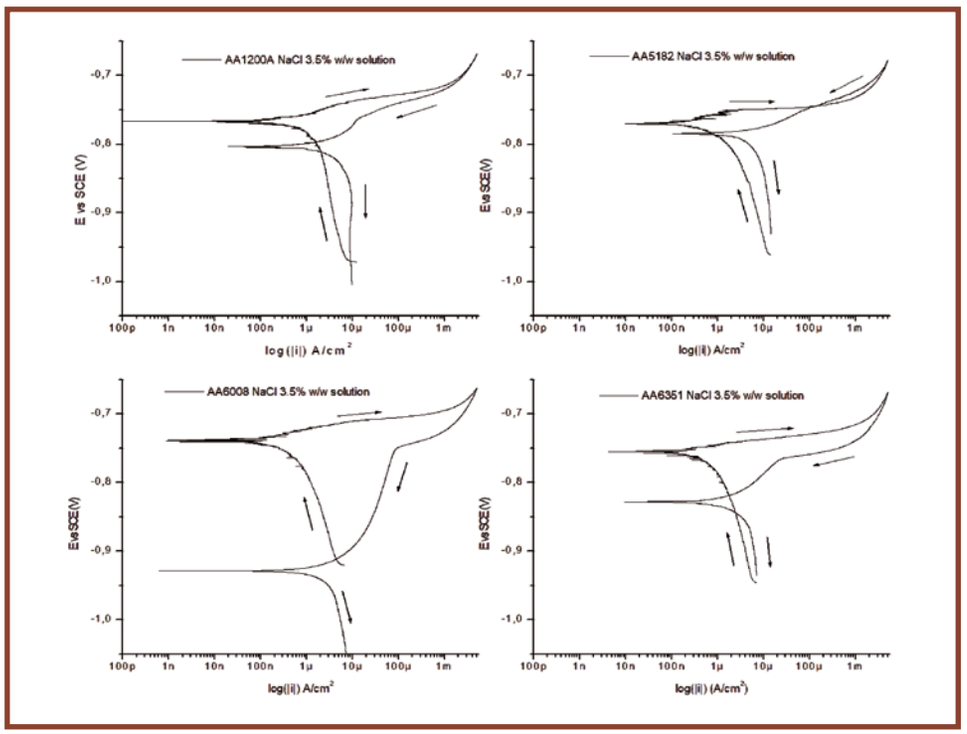

Figure 5 - Tafel plot of the data collected from CPP in aerated 3.5% NaCl solution. Arrows indicate the potential scan direction.

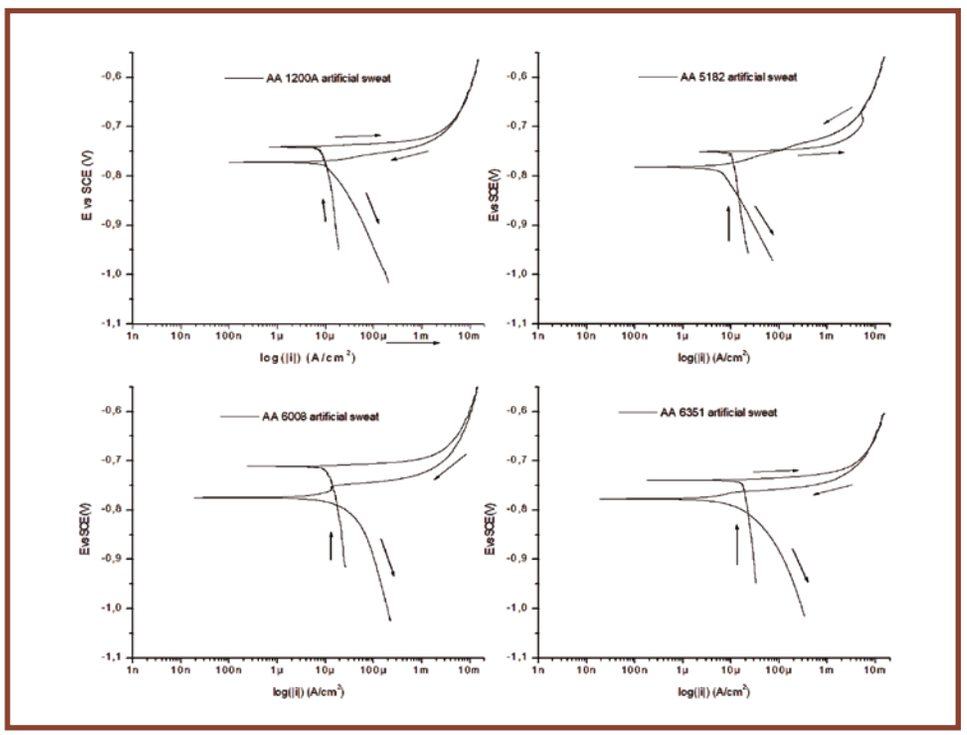

Figure 6 - Tafel plot of the data collected from CPP in artificial sweat solution. Arrows indicate the potential scan direction.

However, also in this environment, AA5182 alloy resulted the less affected by corrosion phenomena.

Cyclic potentiodynamic polarisation tests

The cyclic potentiodynamic polarisation curves performed in the neutral saline environment are depicted in **Figure 5**, while the ones collected in artificial sweat are represented in **Figure 6**. It is worth noting that, among the tested alloys, there are significant differences in the backward scan. In saline neutral environment repassivation and pit transition potentials are located some tenth of mV far from each other, while in artificial sweat solution their value is almost coincident. Going into more detail, the forward scan of the cycled polarisations depicted in figure 5 show modest differences among the tested alloys. The E_{corr} and E_{pit} values fall within a 30mV range, giving poor information about the alloy's stability in this environment. The value of pit transition, passivation and the secondary corrosion potentials were similar, but despite this closeness, their relative position confers to the entire scan a well differentiated shape. Regarding the hysteresis, all the tested alloys but AA5182 presented a positive loop.

The shape of the CPP curves registered in artificial sweat present peculiarities respect the curves collected in neutral saline environment as highlighted by the example depicted in **Figure 7** which, for the same alloy (AA6008) the CPP curves are compared. It is evident as in artificial sweat pitting and corrosion potentials coincides (see Figures 6 and 7). Moreover, the curves collected in artificial sweat presented a well differentiated reverse scan, showing values that are close only for pit transition potential and for the hysteresis sign. E_{rp} and E_{ptp} are relatively close each other except in the case of AA5182, and the corrosion phenomena take place at more cathodic values that, albeit different, are closer to the repassivation potential with respect to the ones determined in neutral saline solution.

SEM and optical investigation of corroded samples

During exposure tests in the neutral saline environment, corrosion byproducts tend to accumulate on the surface leading to the formation of deposits which can occlude the pits (**Figure 8**). AA6351 behaves similarly to AA6008, while AA1200A is characterised by a larger number of surface cracks with only small pits. AA5182 presents an almost undamaged surface.

Vice versa, in acidic environment, the amount of saline byproducts was dramatically reduced. AA6008 displayed the largest corrosion degree characterised by the presence of two distinct corrosion features: a) highly fractured layer and b) deeply eroded portions of the surface (**Figure 9**). Similar features were displayed by AA6351, while the AA1200A alloy presents tiny pits and the AA5182 results mostly unaffected by corrosion phenomena.

Discussion and conclusions

As evidenced in the previous paragraph the complex behaviour of the passive layer makes the use of $E_{corr,}$ E_{pit} and OCP alone insufficient to correctly predict the alloy sensitivity to localised corrosion susceptibility. To overcome this issue, delta potentials values, which are achievable from CPP tests, have been extensively studied in the last 50 years. In particular we focus on a serie of deltas as defined in the following: a) $\Delta E_{ps} = (E_{bd(pit)} - E_{ptp})$ [21] (we named it pitting stable (ps)), that represent the potential range from the pitting outbreak until the point of repassivation due to the occlusion of the pits via accumulation of corrosion byproducts; b) $\Delta E_{pp}=(E_{bd(pit)} - E_{rp})$ [23] (we named it pit progression (pp)), that is the potential span from the pitting outbeak to the point of surface repassivation; c) $\Delta E_{corr} = (E_{corr}$ and $E_{seccorr})$[28] (we named it corrosion's delta), determined as the difference between the corrosion potentials in the forward and the backward scan; d) $\Delta E_{pspe} = (E_{corr}$ and $E_{rp})$ (we named it pitting start - pitting end (pspe)),

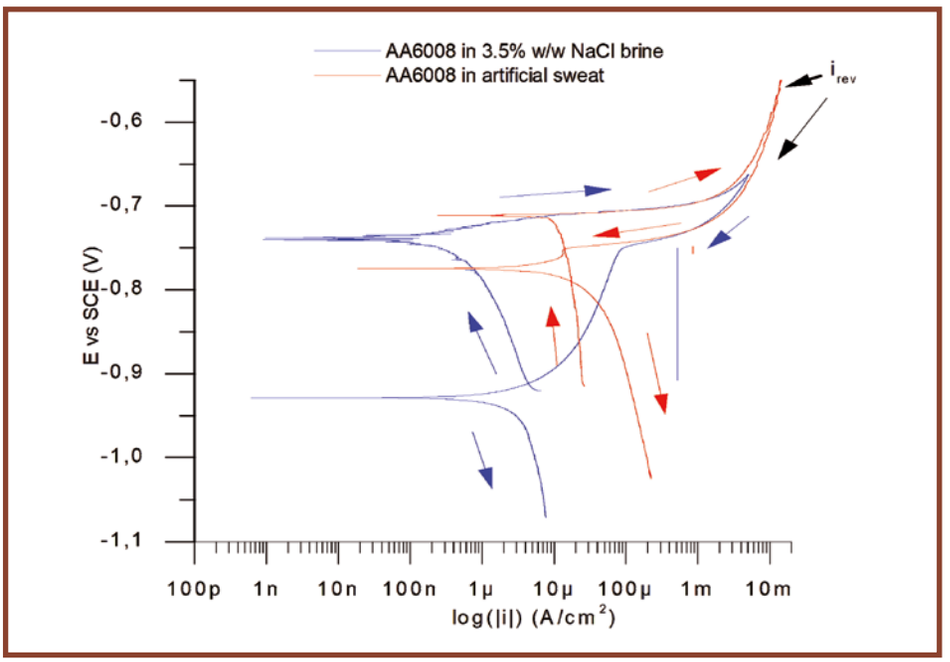

Figure 7 - CPP of AA6008 performed in neutral NaCl solution (blue line) and artificial sweat (red line). Moving from neutral to acidic environment makes the pitting and corrosion potentials to coincide and the entire curve shifts to higher current's values.

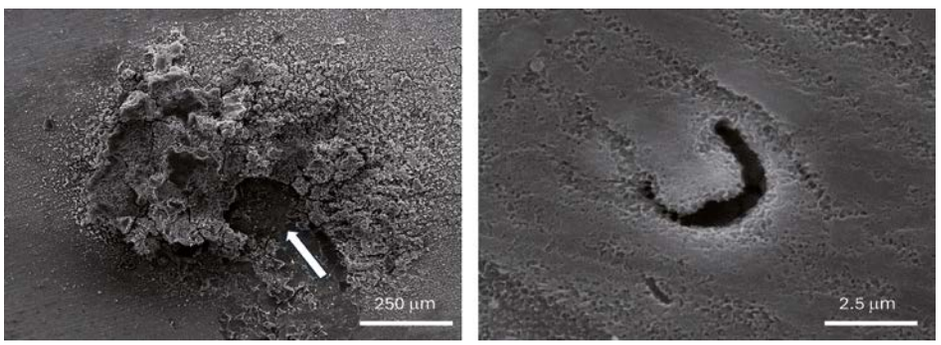

Figure 8 - Corrosion pit on AA6008 after 4 weeks of exposure to salt spray test. (left) The pit is not completely occluded by the corrosion by products (ruler 250 µm). (right) A small open pit free of deposits (ruler 2.5 µm).

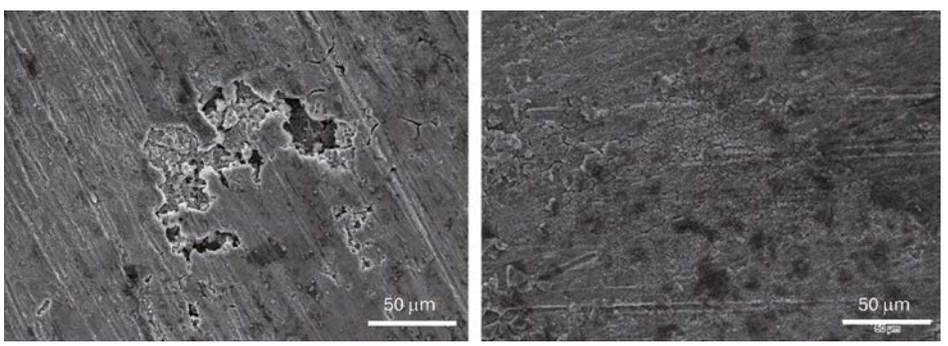

Figure 9 - SEM Images of different parts of AA6008 surface showing IGC features (left), and cracked oxide layers (right). Ruler = 50 µm.

Alloy	ΔE_{ps} NaCl (mV)	ΔE_{ps} a.s. (mV)	ΔE_{pp} NaCl (mV)	ΔE_{pp} a.s. (mV)	ΔE_{pspe} NaCl (mV)	ΔE_{corr} NaCl (mV)	ΔE_{corr} a.s. (mV)	Hysteresis sign
AA1200A	+16 ± 2	+15 ± 1	+57 ± 2	+29 ± 1	+42 ± 2	+51 ± 2	+30 ± 1	+
AA5182	-9 ± 1	-15 ± 2	-8 ± 1	-10 ± 3	-27 ± 2	+31 ± 2	+30 ± 3	-
AA6008	+32 ± 2	+41 ± 1	+198 ± 8	+46 ± 5	+188 ± 4	+211 ± 7	+63 ± 2	+
AA6351	+26 ± 3	+28 ± 2	+84 ± 8	+27 ± 3	+74 ± 2	+81 ± 2	+39 ± 2	+

Table 2: Delta values determined via CPP in the two test solutions. $\Delta E_{ps} = (E_{bd(pit)} - E_{ptp})$, $\Delta E_{pp} = (E_{bd(pit)} - E_{rp})$, $\Delta E_{corr} = (E_{corr}$ and $E_{seccorr})$, $\Delta E_{pspe} = (E_{corr} - E_{rp})$, NaCl stands for 3.5% sodium chloride, a.s. stands for artificial sweat.

the range of potentials from pitting from onset as a metastable phenomenon until the surface repassivation potential.
The experimental value of these parameters are summarized in **Table 2**.
We also account the hysteresis sign as positive the one formed after current's increase following the scan reversal (see Figure 6A for a positive sign and Figure 6B for a negative one). The positive sign has been interpreted as associated to the localised corrosion attack and the negative one as the substantial protection against this phenomenon. The identified ΔE trace back their meaning to a physical interpretation, some are identified by the mixed potential theory (corrosion and secondary corrosion potentials), others are more related to the corrosion mechanism (pitting, breakdown, pit transition etc) or surface passive layer restoration (E_{rp}). Pitting potential is dependent on the state of the passivating layer with little regard to its thickness [30] but it is strictly dependent upon chemical stability in such an environment as assessed by Galvele's equation [31]. Since pitting may initiate via a metastable mechanism above the E_{corr}, the E_{pit} is the value beyond which pitting becomes a self-sustaining mechanism. On the other hand, E_{ptp} is the potential at which, during the reverse scan, an abrupt slope's change can be detected in the semilogarithmic plot that is reasonably related to the inhibition of the charge transfer mechanism, taking place inside the sites of localised attack and expressed by the potential in Newman's equation [13]. In this interpretation, at potential below than E_{ptp} the pits cannot form but, if already present, they can propagate, until reaching the repassivation potential (E_{rp}) where pits cannot growth.
Indeed, the superior corrosion resistance displayed by AA5182 in neutral NaCl solution is also well represented by the sign of the hysteresis loop. Moving from neutral to acidic, and more complex solutions, AA5182 still remains the most performing alloys but the number of truthful parameters dramatically decrease; only the ΔE_{ps} still correlates to the observed corrosion damage. Regarding the superior performance displayed by AA5182 respect to local corrosion, it can reasonably be related to its relatively high magnesium content (see table 1). The possible formation of more stable magnesium hydroxide can account for the occurrence of pit transition and repassivation at potentials that are higher than the breakdown potential one. It is possible to propose an acid base reaction between magnesium oxide/hydroxide during the recording of the cyclic potentiodynamic polarisation after current reversal in the portion of the scan that is characterised by the hysteresis loop. This reaction may stop the acidification of the surface that several authors identified as the responsible for the hysteresis loop [26] reducing the sensitivity of the AA5182 alloy even in acidic environment.
Electrochemical and free corrosion tests in acidic and neutral saline environments on four different aluminium alloys evidenced that the relative stability of the "as formed" passive layer is not the key point in guarantee the protection of the material but, vice versa, the capability of the layer to repassivate become a pivotal attribute. That can be accounted via both, pores occlusion or the formation of a new passive layer. Noteworthy, and in accordance with previous work [32], E_{ptp} value is almost unaffected by the environment, letting to assess that it is mainly related to the composition of the alloy and the peculiar chemistry of the cavities microenvironment [33].

References

[1] ISO 9227:2022, corrosion tests in artificial atmospheres.

[2] ISO 3160-2 Watch cases and accessories, Gold alloy coverings, Part 2: Determination of fineness, thickness, corrosion resistance and adhesion.

[3] ASTM G46-21 Standard Guide for Examination and Evaluation of Pitting Corrosion.

[4] R. G. Kelly, "pitting corrosion",in " Corrosion tests and standards: application and interpretation", ed. Second, R. Baboian (ed.), ASTM international, Philadelphia, PA 2005, 166-174.

[5] ASTM G61-86 Standard Test Method for Conducting Cyclic Potentiodynamic Polarization Measurements for Localized Corrosion Susceptibility of Iron-, Nickel-, or Cobalt-Based Alloys.

[6] ASTM G199-09 Standard Guide for Electrochemical Noise Measurement.

[7] ASTM G106-89 Standard Practice for Verification of Algorithm and Equipment for Electrochemical Impedance Measurements.

[8] ASTM G59-97 Standard Test Method for Conducting Potentiodynamic Polarization Resistance Measurements, 2020.

[9] ASTM G192-08 Standard Test Method for Determining the Crevice Repassivation Potential of Corrosion-Resistant Alloys Using a Potentiodynamic-Galvanostatic-Potentiostatic Technique.

[10] R. G. Kelly, et al., "Passivity and localized corrosion", in "Electrochemical techniques in corrosion science and engineering". Marcel Dekker inc., 2002, 55-123.

[11] ASTM G5-14 Standard Reference Test Method for Making Potentiodynamic Anodic Polarization Measurements.

[12] R. C. Newman, "Local chemistry considerations in the tunnelling corrosion of aluminium" Corros Sci. vol 37, 3, pp. 527-533, 1995

[13] N.J. Laycock, R. C. Newman, "Localised dissolution kinetics, salt films and pitting potentials" Corros. Sci. vol 39, 10-11, pp 1771-1790, 1997

[14] Q. Sun, K. Chen, "Inflection of backward sweep of cyclic polarization curve: Pit transition potential E ptp" Mater. Corros. Vol 69, 12 pp 1729–1740, 2018.

[15] D. Cicolin, M. Trueba, S. P. Trasatti, "Effect of chloride concentration, pH and dissolved oxygen, on the repassivation of 6082-T6 Al alloy" Electrochim. Acta vol 124, pp 27-35, 2014.

[16] S. T. Pride, J. R. Scully, J. L. Hudson, "Metastable pitting of aluminum and criteria for the transition to stable pit growth" J. Electrochem. Soc. vol141, 11, pp 3028-3040, 1994.

[17] N. Sridhar, G.A. Cragnolino, "Applicability of Repassivation Potential for Long-Term Prediction of Localized Corrosion of Alloy 825 and Type 316L Stainless Steel" Corros., vol 49, 11, pp 885-894, 1993.

[18] Z. Szklarska-Smialowska, "Pitting corrosion of aluminium" Corros. Sci. vol. 41, 9, pp 1743-1767, 1999.

[19] S. Esmailzadeh, M. Aliofkhazraei, H. Sarlak, "Interpretation of Cyclic Potentiodynamic Polarization Test Results for Study of Corrosion Behavior of Metals: A Review" Prot. Met. Phys. Chem. Surf. Vol 54, 5, pp 976–989, 2018.

[20] M. Zakeri, et al, "Pit Transition Potential and Repassivation Potential of Stainless Steel in Thiosulfate Solution" J. Electrochem. Soc. Vol 163, 6, C275-C281, 2016.

[21] M. Trueba, S. P. Trasatti, "Study of Al alloy corrosion in neutral NaCl by the pitting scan technique" Mat. Chem. Phys. Vol 121, 3, pp 523-533, 2010

[22] N. Nilsen, E. Bardal, "Short duration tests and a new criterion for characterization of pitting resistance of Al alloys" Corros. Sci. 17, 8 , 635-646, 1977.

[23] B. E. Wilde, E. Williams, "The relevance of accelerated electrochemical pitting tests to the long- term pitting and crevice corrosion behavior of stainless steels in marine environments" J. Electrochem. Soc. Vol 118, 7, pp 1057- 1062, 1971.

[24] E. Melilli, M. Trueba, S. P. Trasatti, Effect of chloride concentration on the repassivation behavior of structural Al alloys Metall. Ital. 106, pp 29-33, 2014.

[25] B. Zaid, D. Saidi, A. Benzaid, S. Hadji, Effects of pH and chloride concentration on pitting corrosion of AA6061 aluminum alloy., Corros. Sci. vol 50, 7,pp 1841-1847, 2008.

[26] W. Zhang, G. S. Frankel, "Transitions between pitting and intergranular corrosion in AA2024" Electrochim. Acta vol48, 9, pp 1193-1210, 2003.

[27] K. L. Moore, J. M. Sykes, P. S. Grant, "An electrochemical study of repassivation of aluminium alloys with SEM examination of the pit interiors using resin replicas" Corros. Sci. vol 50, 11, 3233-3240, 2008.

[28] Q. Sun, K. Chen, "Effect of scan rate on polarization curves of a high strength Al alloy in 3.5 wt% NaCl solution" J. Electrochem. Sci. Technol. vol11, 2, pp140-147, 2020.

[29] M. Yasuda, F. Weinberg, D. Tromans, "Pitting corrosion of Al and Al- Cu single crystalsJ. Electrochem", Soc. Vol 137, 12, pp 3708-3715, 1990.

[30] J. Soltis, "Passivity breakdown, pit initiation and propagation of pits in metallic materials–review", Corros. Sci. Vol 90, pp5-22, 2015.

[31] J. R. Galvele, "Transport processes and the mechanism of pitting of metals" J. Electrochem. Soc. Vol123, 4, pp 464-474, 1976.

[32] I. M. Comotti, M. Trueba, S. P. Trasatti, "The pit transition potential in the repassivation of aluminium alloys" Surf. Interf. Anal. Vol 45, 10, pp 1575-1584, 2013.

[33] M. Trueba, S. P. Trasatti, "Electrochemical approach to repassivation kinetics of Al alloys: gaining insight into environmentally assisted cracking" Corros. Rev. Vol33, 6, pp373-393, 2015.